

PRETRAIN-DPFL: MITIGATING NOISE DETRIMENT IN DIFFERENTIALLY PRIVATE FEDERATED LEARNING WITH MODEL PRE-TRAINING

Huitong Jin¹ Yipeng Zhou² Quan Z. Sheng² Shiting Wen³ Laizhong Cui^{1*}

¹ Shenzhen University, China ² Macquarie University, Australia ³ NingboTech University, China

ABSTRACT

Differentially Private Federated Learning (DPFL) strengthens privacy protection by perturbing model gradients with noise, though at the cost of reduced accuracy. Although prior empirical studies indicate that initializing from pre-trained rather than random parameters can alleviate noise disturbance, the problem of optimally fine-tuning pre-trained models in DPFL remains unaddressed. In this paper, we propose Pretrain-DPFL, a framework that systematically evaluates three most representative fine-tuning strategies: full-tuning (FT), head-tuning (HT), and unified-tuning(UT) combining HT followed by FT. Through convergence analysis under smooth non-convex loss, we establish theoretical conditions for identifying the optimal fine-tuning strategy in Pretrain-DPFL, thereby maximizing the benefits of pre-trained models in mitigating noise disturbance. Extensive experiments across multiple datasets demonstrate Pretrain-DPFL’s superiority, achieving 25.22% higher accuracy than scratch training and outperforming the second-best baseline by 8.19%, significantly improving the privacy-utility trade-off in DPFL.

Index Terms— Differential Privacy, Federated Learning, Model Pre-training, Noise Mitigation, Fine-tuning Strategies.

1. INTRODUCTION

Differentially Private Federated Learning (DPFL) is the de facto standard privacy preservation framework for model training across multiple clients [1, 2]. DPFL improves Federated Learning (FL) by adding Gaussian [3] or Laplace [4] noise to gradients to protect privacy, though at the cost of model performance degradation [5, 6]. Previous efforts have been dedicated to mitigating Differentially Private (DP) noise influence by developing specialized architectures for private training [7, 8], or reducing model size during training [9, 10].

* Corresponding author: cuilz@szu.edu.cn

This work has been partially supported by National Natural Science Foundation of China under Grant No. U23B2026 and No.62372305, Guangdong Basic and Applied Basic Research Foundation under Grant No. 2024B1515040012, Shenzhen Science and Technology Program under Grant No. KJZD20230923114809020, and Research Team Cultivation Program of Shenzhen University, Grant No.2023QNT015 and Key Programs of Ningbo Municipal Natural Science Foundation Under Grant No. 2024J021.

Orthogonal to existing methods, DP fine-tuning approaches leveraging pre-training models to boost DPFL have recently garnered increasing attention[11, 12]. DP fine-tuning typically begins with a pre-trained model obtained from training on public datasets (e.g., ImageNet-1K) without privacy constraints, followed by private fine-tuning on specific downstream datasets (e.g., CIFAR-10) [13]. Recent studies reported that the use of pre-trained parameters in DPFL can accelerate model convergence, reduce model exposure times, and hence mitigate noise influence, compared to scratch training (ST) which begins with randomly initialized parameters [11, 14, 15, 16]. In particular, [14] has empirically tried different fine-tuning strategies, such as head-tuning (HT) and full-tuning (FT). [16] proposed unified-tuning (UT) that first HT followed by FT and theoretically derived the performance gaps between HT, FT, and UT under varying noise scales. However, these studies primarily focus on Machine Learning (ML) scenarios without specifying the optimal fine-tuning strategy under different conditions. In particular, [16] explored the optimal fine-tuning strategy by simultaneously attempting different strategies. This approach is impractical in DPFL, as it would lead to a multiplicative privacy budget consumption due to the exposure of gradients in each attempt.

To identify the optimal fine-tuning strategy in DPFL with pre-trained models, we introduce the Pretrain-DPFL framework, one of the first approaches capable of automatically selecting the optimal strategy. From a learning perspective, FT is expected to outperform HT, as HT updates only a small portion of model parameters (i.e., a few layers). From a privacy perspective, however, HT incurs significantly lower privacy loss than FT, since only the fine-tuned parameters are exposed. Balancing these competing factors makes it challenging to determine the optimal strategy in practical DPFL. To address this challenge, we formalize the UT strategy that conducts T_1 rounds of HT followed by $T - T_1$ rounds of FT, where T is the total number of model exposure rounds. We analyze the convergence of this unified strategy under smooth non-convex loss, through which we can quantify the performance gap between FT and HT under different conditions, and further determine the best strategy with the optimal T_1 .

In summary, our contributions are three-fold. *Firstly*, we analyze the convergence of HT, FT, and UT under smooth non-convex loss and derive conditions for selecting the opti-

mal strategy. *Secondly*, we propose the Pretrain-DPFL framework, which automatically selects the optimal fine-tuning strategy for DPFL without incurring additional privacy cost from trial-and-error tuning. *Lastly*, extensive experiments on multiple datasets show that Pretrain-DPFL improves accuracy by 25.22% over ST and 8.19% over the second-best baseline under a fixed privacy budget.

2. PRELIMINARIES

2.1. Differential Privacy

Definition 1. *(ϵ, δ) -Differential Privacy [6]:* A randomized algorithm \mathcal{M} satisfies (ϵ, δ) -DP if for any two datasets \mathcal{D} and \mathcal{D}' differing by one element, and for any subset \mathcal{S} of outputs:

$$\Pr[\mathcal{M}(\mathcal{D}) \in \mathcal{S}] \leq \exp(\epsilon) \Pr[\mathcal{M}(\mathcal{D}') \in \mathcal{S}] + \delta, \quad (1)$$

Here, ϵ is the privacy budget and δ is the failure probability; smaller values indicate stronger privacy.

2.2. DPFL with Different Fine-tuning Strategies

We adopt FedSGD as the DPFL framework[17, 18] with N clients jointly training global model $F(\theta)$, where $\theta \in \mathbb{R}^{p+n}$ includes with feature extractor(\mathbb{R}^p) and classifier head (\mathbb{R}^n). we formally define the three fine-tuning strategies:

Definition 2. Head-Tuning Strategy (HT): Only the last n parameters are trainable. After local updates and aggregation, the global update at iteration t is: $\hat{\theta}_{t+1} = \sum_{i=1}^N \frac{d_i}{d} [\hat{\theta}_t - \eta_t (\mathbf{m} \odot \mathbf{g}_t^i + \tilde{\mathbf{w}}_t^i)] = \hat{\theta}_t - \eta_t (\mathbf{m} \odot \mathbf{g}_t + \tilde{\mathbf{w}}_t)$.

Here, η_t is the learning rate, $\mathbf{m} = [0_p, 1_n]^T$ masks the gradient, $\mathbf{g}_t = \sum_{i=1}^N \frac{d_i}{d} \mathbf{g}_t^i$ is the aggregated gradient, and $\tilde{\mathbf{w}}_t = \sum_{i=1}^N \frac{d_i}{d} \tilde{\mathbf{w}}_t^i$ represents the aggregated DP noise.

Definition 3. Full-Tuning Strategy (FT): All $p + n$ parameters are trainable. After local updates and aggregation, the global update at iteration t is: $\hat{\theta}_{t+1} = \sum_{i=1}^N \frac{d_i}{d} [\hat{\theta}_t - \eta_t (\mathbf{g}_t^i + \tilde{\mathbf{w}}_t^i)] = \hat{\theta}_t - \eta_t (\mathbf{g}_t + \hat{\mathbf{w}}_t)$.

Here, $\hat{\mathbf{w}}_t^i \in \mathbb{R}^{p+n}$ represents the DP noise added by client i , and $\hat{\mathbf{w}}_t = \sum_{i=1}^N \frac{d_i}{d} \hat{\mathbf{w}}_t^i$ denotes the aggregated noise.

Definition 4. Unified-Tuning Strategy (UT): Suppose that DPFL will conduct T global iterations. The UT strategy consists of two phases: the first T_1 ($0 < T_1 < T$) iterations of HT, followed by $T - T_1$ iterations of FT.

In our analysis, we will study how to set T_1 for determining the optimal fine-tuning strategy.

3. PRETRAIN-DPFL FRAMEWORK

3.1. Pretrain-DPFL

The DPFL using pre-trained parameters (Pretrain-DPFL) framework is presented in Algorithm 1. Firstly, model pa-

Algorithm 1 Pretrain-DPFL FrameWork

```

1: Step 1: Pretrain on ImageNet-1K to obtain  $\theta_0$ .
2: Step 2: Estimate  $G_1^2, G_2^2, \Lambda_1^2, \Lambda_2^2, L, \Gamma$  from clients.
3: Step 3: Compute  $T_1$  based on Theorem 2 or 3.
4: Step 4: Main training
5: for each round  $t = 0, \dots, T - 1$  do
6:   for each client  $i$  do
7:     Sample batch  $\mathcal{B}_t^i$  from  $\mathcal{D}_i$ .
8:     Generate  $\tilde{\mathbf{w}}_t^i$  (or  $\hat{\mathbf{w}}_t^i$ ) accoding to DP mechanism.
9:   Update parameters as follows


$$\theta_{t+1}^i = \begin{cases} \theta_t^i - \eta_t (\mathbf{m} \odot \nabla F_i + \tilde{\mathbf{w}}_t^i), & t \leq T_1 \text{ (HT)} \\ \theta_t^i - \eta_t (\nabla F_i + \hat{\mathbf{w}}_t^i), & t > T_1 \text{ (FT)} \end{cases}$$


10:  end for
11:  Server aggregates:  $\theta_{t+1} = \sum_{i=1}^N \frac{d_i}{d} \theta_{t+1}^i$ 
12: end for

```

rameters are pretrained on a public dataset (e.g., ImageNet-1K [19]) in a centralized manner on the server, yielding the initialization θ_0 . Secondly, each client locally estimates $G_1^2, G_2^2, \Lambda_1^2, \Lambda_2^2, L$, and Γ using the algorithm proposed in [18, 20, 21], and transmits the results to the server, which then aggregates them to obtain the final global estimates. Based on the aggregated values, the server computes T_1 according to Theorem 2 or Theorem 3. Finally, the training proceeds for T global rounds: each client samples a minibatch, adds DP noise accoding to DP mechanism, and updates local parameters under either HT or FT strategy depending on $t \leq T_1$ or $t > T_1$. The server aggregates the updates to obtain the global model. In this way, Pretrain-DPFL adaptively selects the optimal fine-tuning strategy, ensuring that the model achieves the best utility-privacy performance.

Specifically, Step 2 incurs only minimal overhead: each client requires few iterations (set to 5 in our experiments) to obtain the statistics, leading to an additional time cost of less than 10%. Moreover, only 6 scalar values are transmitted to the server, resulting in $\mathcal{O}(1)$ communication cost. Compared with sharing gradients or model weights, these statistics reveal negligible private information. For additional safety, we allocate a privacy budget of 0.01 to protect the reported statistics, thereby further strengthening privacy guarantees.

3.2. Theoretical Analysis

In DPFL, the injected noise $\tilde{\mathbf{w}}_t^i$ and $\hat{\mathbf{w}}_t^i$ follow Laplace or Gaussian mechanisms. We briefly summarize key definitions and assumptions before presenting the convergence theorems.

Theorem 1. Laplace Mechanism [4]. For a query with the l_1 -sensitivity, assuming that gradients are l_1 -bounded by ξ_1 , the Laplace mechanism ensures $(\epsilon_i, 0)$ -DP by adding $\tilde{\mathbf{w}}_t^i \sim \text{Lap} \left(0, \frac{2T\xi_1}{d_i \epsilon_i} \mathbb{I}_n \right)$, $\hat{\mathbf{w}}_t^i \sim \text{Lap} \left(0, \frac{2T\xi_1}{d_i \epsilon_i} \mathbb{I}_{p+n} \right)$.

Proposition 1. *Variance of aggregated Laplace noise: The expected L_2 -norm squared of the aggregated Laplace noise over N clients is: $\mathbb{E}[\|\tilde{\mathbf{w}}_t\|_2^2] = \frac{8nT^2\xi_1^2}{d^2} \sum_{i=1}^N \frac{1}{\epsilon_i^2}$ for HT or $\mathbb{E}[\|\hat{\mathbf{w}}_t\|_2^2] = \frac{8(p+n)T^2\xi_1^2}{d^2} \sum_{i=1}^N \frac{1}{\epsilon_i^2}$ for FT.*

Definition 5. *The Bound of Non-IID Degree [9]: For any model θ , we define $\Gamma \geq \mathbb{E}[\|\nabla F_i(\theta) - \nabla F(\theta)\|_2^2]$.*

Assumption 1. *L -smoothness [22]: All local loss functions F_i are L -smooth, i.e., for any $\theta, \theta' \in \mathbb{R}^{p+n}$, we have $F_i(\theta) \leq F_i(\theta') + \langle \nabla F_i(\theta'), \theta - \theta' \rangle + \frac{L}{2} \|\theta - \theta'\|_2^2$, for $i = 1, \dots, N$.*

Assumption 2. *Bounded variance and second moment [9]: For any $\theta \in \mathbb{R}^n$ with $t \geq 1$, there exist constants $\Lambda_1, \Lambda_2 > 0$ and $G_1 \geq \Lambda_1, G_2 \geq \Lambda_2$ such that $\mathbb{E}_{\mathcal{B}_t \subset \mathcal{D}_i} [\|\nabla F_i(\theta; \mathcal{B}_t) - \nabla F_i(\theta)\|_2^2] \leq \Lambda_j^2$ and $\mathbb{E}_{\mathcal{B}_t \subset \mathcal{D}_i} [\|\nabla F_i(\theta; \mathcal{B}_t)\|_2^2] \leq G_j^2$, for $\theta = \hat{\theta}_{t-1}$ ($j = 1$) and $\theta = \hat{\theta}_{t-1}$ ($j = 2$).*

Let v_t denote FT parameters after t rounds without noise. Based on the Assumption 2 and Proposition 1, we derive:

Lemma 1. *Bounding the Distance Between Noisy HT and Noise-Free FT Parameters under Laplace Mechanism:*

$$\mathbb{E}[\|v_t - \tilde{\theta}_t\|_2^2] \leq 2\eta^2[2(G_1^2 + G_2^2) + \frac{8nT^2\xi_1^2}{d^2} \sum_{i=1}^N \frac{1}{\epsilon_i^2}]. \quad (2)$$

Lemma 2. *Bounding the Distance Between Noisy and Noise-Free FT Parameters under Laplace Mechanism:*

$$\mathbb{E}[\|v_t - \hat{\theta}_t\|_2^2] \leq \eta^2(\frac{8(n+p)T^2\xi_1^2}{d^2} \sum_{i=1}^N \frac{1}{\epsilon_i^2}). \quad (3)$$

Theorem 2. *Let Assumptions 1 and 2 hold. Let the learning rate $\eta = \frac{\beta}{\sqrt{T}}$ where $\beta < \frac{\sqrt{T}}{2L}$. The convergence rate of Pretrain-DPFL under the Laplace Mechanism is as follows:*

$$\begin{aligned} & \mathbb{E}[\|\nabla F(\mathbf{x}_T)\|_2^2] \\ &= \frac{1}{T}(\sum_{t=0}^{T_1} \mathbb{E}[\|\nabla F(\tilde{\theta}_t)\|_2^2] + \sum_{t=T_1+1}^T \mathbb{E}[\|\nabla F(\hat{\theta}_t)\|_2^2]) \quad (4) \\ &\leq C_0 + C_1 T_1 + C_2(T - T_1), \end{aligned}$$

where $C_0 = \frac{4\{\mathbb{E}[F(\theta_0)] - F^*\}}{\beta T^{1/2}} + (\frac{64\beta^2 L^2 n \xi_1^2}{d^2} \sum_{i=1}^N \frac{1}{\epsilon_i^2})T$, $C_1 = \frac{4\beta}{T^{3/2}}(\frac{L\Lambda_1^2}{N} + 2L\Gamma) + \frac{16\beta^2 L^2}{T^2}(G_1^2 + G_2^2)$, and $C_2 = \frac{4\beta}{T^{3/2}}(\frac{L\Lambda_2^2}{N} + 2L\Gamma) + \frac{64\beta^2 L^2 p \xi_1^2}{d^2} \sum_{i=1}^N \frac{1}{\epsilon_i^2}$.

We sketch the proof of Theorem 2 as follows. Under the given assumptions, we first obtain $\mathbb{E}[F(v_{t+1})] - F(v_t) \leq -\frac{\eta}{4} \|\nabla F(\tilde{\theta}_t)\|_2^2 + \eta L^2 \|v_t - \tilde{\theta}_t\|_2^2 + 2L\eta^2\Gamma + \frac{L\eta^2\Lambda_1^2}{N}$. By applying Lemma 1 and taking expectations, we can bound $\mathbb{E}[\|\nabla F(\tilde{\theta}_t)\|_2^2]$. Similarly, invoking Lemma 2 allows us to bound $\mathbb{E}[\|\nabla F(\hat{\theta}_t)\|_2^2]$. Summing over all iterations and simplifying yields the desired result for $\mathbb{E}[\|\nabla F(\mathbf{x}_T)\|_2^2]$.

The main insights from Theorem 2 include: (1) In the absence of noise, all terms vanish as $T \rightarrow \infty$, ensuring convergence. (2) By ignoring Λ_1 and Λ_2 , the magnitudes of C_1 and C_2 are primarily determined by $\frac{16\beta^2 L^2}{T^2}(G_1^2 + G_2^2)$ and $\frac{64\beta^2 L^2 p \xi_1^2}{d^2} \sum_{i=1}^N \frac{1}{\epsilon_i^2}$, respectively.¹ The former represents the learning capability gap between HT and FT, while the latter reflects the additional noise impact of FT by tuning p more parameters. (3) For fixed ϵ and T , the optimal T_1 minimizing $\mathbb{E}[\|\nabla F(\mathbf{x}_T)\|_2^2]$ can be identified: if $C_1 \geq C_2$, the optimal configuration is $T_1 = T$, indicating that *the HT fine-tuning strategy should be selected*. Conversely, when $C_1 < C_2$, the optimal choice is $T_1 = 0$, suggesting that *the FT fine-tuning strategy should be adopted*.

We extend the analysis of the previous section to the Gaussian mechanism [3], where gradients are l_2 -bounded by ξ_2 , and noise $\tilde{\mathbf{w}}_t^i \sim \mathcal{N}(0, \sigma_i^2 \mathbb{I}_n)$, $\hat{\mathbf{w}}_t^i \sim \mathcal{N}(0, \sigma_i^2 \mathbb{I}p + n)$ are added with variance $\sigma_i^2 \geq \frac{c_2^2 \xi_2^2 T}{d_i^2 \epsilon_i^2} \log \frac{1}{\delta_i}$.

Theorem 3. *Let Assumptions 1 and 2 hold. Let the learning rate $\eta = \frac{\beta}{\sqrt{T}}$ where $\beta < \frac{\sqrt{T}}{2L}$. The convergence rate of Pretrain-DPFL under the Gaussian Mechanism is as follows:*

$$\begin{aligned} & \mathbb{E}[\|\nabla F(\mathbf{x}_T)\|_2^2] \\ &= \frac{1}{T}(\sum_{t=0}^{T_1} \mathbb{E}[\|\nabla F(\tilde{\theta}_t)\|_2^2] + \sum_{t=T_1+1}^T \mathbb{E}[\|\nabla F(\hat{\theta}_t)\|_2^2]) \quad (5) \\ &\leq E_0 + E_1 T_1 + E_2(T - T_1), \end{aligned}$$

where $E_0 = \frac{4\{\mathbb{E}[F(\theta_0)] - F^*\}}{\beta T^{1/2}} + \frac{8\beta^2 L^2 c_2^2 n \xi_2^2}{d^2} \sum_{i=1}^N \frac{1}{\epsilon_i^2} \log \frac{1}{\delta_i}$, $E_1 = \frac{4\beta}{T^{3/2}}(\frac{L\Lambda_1^2}{N} + 2L\Gamma) + \frac{16\beta^2 L^2}{T^2}(G_1^2 + G_2^2)$, and $E_2 = \frac{4\beta}{T^{3/2}}(\frac{L\Lambda_2^2}{N} + 2L\Gamma) + \frac{8\beta^2 L^2}{T^2}(\frac{c_2^2 p \xi_2^2 T}{d^2} \sum_{i=1}^N \frac{1}{\epsilon_i^2} \log \frac{1}{\delta_i})$.

Similarly, Theorem 3 shows that when $E_1 \geq E_2$, FT outperforms HT, whereas when $E_1 < E_2$, HT performs better.

4. EXPERIMENTS

4.1. Experiment Setup

We pretrain on ImageNet-1K [19] and fine-tune on CIFAR-10 [18] (60k color images of size $3 \times 32 \times 32$) and Fashion-MNIST [18] (70k grayscale images of size 28×28). To match the pre-trained backbone, all images are resized to $3 \times 32 \times 32$. Considering data heterogeneity in FL, we partition data across $N=10$ clients using a Dirichlet sampler with $\alpha=1.0$ [23].

We evaluate two models: a CNN with two convolutional and two fully connected layers [9] ($p=543,808$, $n=1,290$), and ResNet20 [24] ($p=1,092,816$, $n=1,290$). The feature extractor is initialized from the ImageNet-1K checkpoint, while the classifier head is initialized using Kaiming initialization [25]. Four fine-tuning strategies are considered:

¹ Λ_1 and Λ_2 can be ignored because $\Lambda_1 \ll G_1$ and $\Lambda_2 \ll G_2$, which can be verified by experiments.

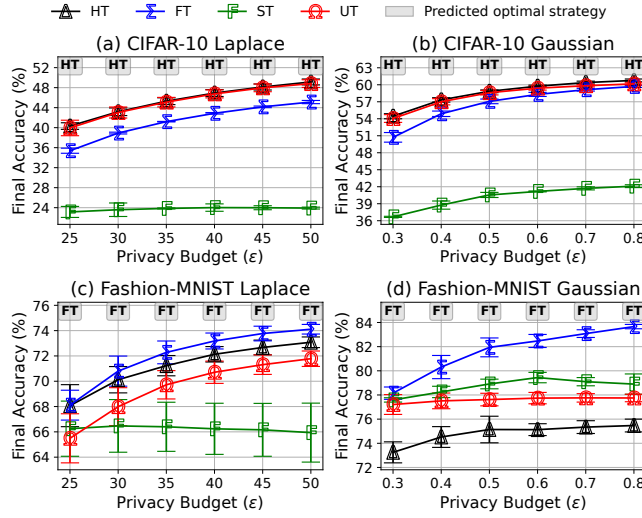


Fig. 1. Comparison of model accuracy across different privacy budgets using a CNN model, with the number of global training iterations set to $T = 128$.

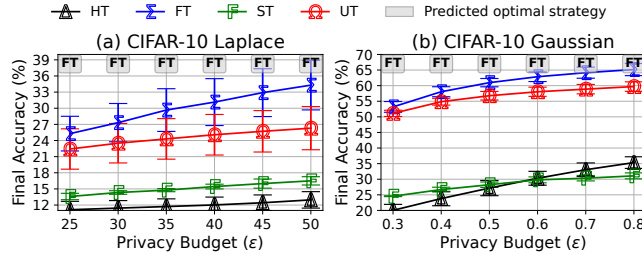


Fig. 2. Comparison of model accuracy across different privacy budgets using a ResNet20 model, with the number of global training iterations set to $T = 128$.

HT, FT, and UT, together with ST (training from scratch) to isolate the effect of pretrained parameters. For UT, we set $T_1 \in \{0.25T, 0.5T, 0.75T\}$ and report results using the best-performing value.

Unless otherwise specified, the total number of global rounds is set to $T=128$. For the Laplace mechanism, gradient clipping bounds are $\xi_1=300$ (CNN) and 50 (ResNet20); for the Gaussian mechanism, the bounds are $\xi_2=15$ (CNN) and 5 (ResNet20) [18]. The privacy budget is assumed identical across clients, i.e., $\epsilon_i=\epsilon$ [9, 18], and the initial learning rate is selected by grid search. Each experiment is repeated three times, and the mean accuracy with error bars is reported.

Finally, according to Theorems 2 and 3, the relative performance of HT and FT depends on the magnitudes of C_1 and C_2 (or E_1 and E_2), which are influenced by ϵ , model architecture, and total iterations T . The subsequent experiments are designed to examine these factors in detail.

4.2. Experiment Results

Effect of privacy budget ϵ . Fig. 1 shows CNN results under Laplace noise ($\delta=0$, $\epsilon \in [25, 50]$) and Gaussian noise

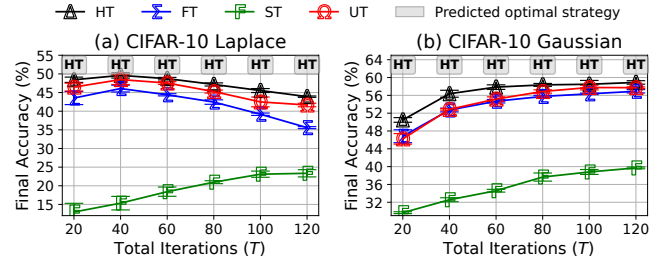


Fig. 3. Comparison of the model accuracy across different total iterations using a CNN model, with the ϵ set to 30 and 0.5 for the Laplace and Gaussian mechanisms, respectively.

($\delta=10^{-5}$, $\epsilon \in [0.3, 0.8]$). (i) The optimal strategies predicted by Pretrain-DPFL are consistent with the empirical winners. For example, under Gaussian noise with $\epsilon=0.8$, FT achieves 83.66% on Fashion-MNIST, outperforming the second-best strategy by 8.19%. (ii) Pretrained fine-tuning methods consistently outperform ST. For instance, under Laplace noise with $\epsilon=50$, HT improves over ST by 25.22% on CIFAR-10.

Impact of architecture. Fig. 2 reports ResNet20 under the same settings. FT generally becomes stronger relative to HT because larger capacity reduces the relative impact of DP noise, which is consistent with the theory analysis.

Effect of total rounds T . Varying $T \in \{20, \dots, 120\}$ (Fig. 3) reveals a utility–privacy trade-off: small T under-utilizes learning, whereas large T amplifies accumulated noise. The predicted strategy remains correct across T , while the best T depends on the privacy mechanism and dataset.

Takeaways. (1) Pretraining markedly improves DPFL utility over ST. (2) The HT vs. FT choice follows the predicted noise–learning balance and varies with ϵ , model, and T . (3) Our selection rule reliably identifies the empirically optimal strategy across settings.

5. CONCLUSION AND FUTURE WORK

As data privacy concerns grow, preserving privacy during model training has gained significant attention. Although DPFL is effective in protecting privacy, its applicability is hindered by the accuracy loss caused by noise. In our pioneering work, we explore how to optimally leverage pre-trained models to mitigate noise influence in DPFL. Specifically, we propose the Pretrain-DPFL framework, which explores the conditions under which the optimal fine-tuning strategy in DPFL can be identified to maximize the advantages of pre-trained models. The superiority of our design is supported not only by rigorous theoretical analysis but also by extensive experiments. The results show that Pretrain-DPFL improves model accuracy by up to 25.22% compared to ST and 8.19% over the state-of-the-art baseline, underscoring its effectiveness in enhancing DPFL. Future work will extend the Pretrain-DPFL framework to broader scenarios, including multi-modal FL, personalized FL, and beyond.

6. REFERENCES

[1] Shenhai Zheng, Congyu Li, Sian Wen, Xi Gao, and Lei Yu, “Cogap: A personalized federated learning method using collaborative optimization for medical image classification,” in *2025 IEEE International Conference on Acoustics, Speech and Signal Processing (ICASSP)*, 2025, pp. 1–5.

[2] Vasileios Tsouvalas, Aaqib Saeed, Tanir Ozcelebi, and Nirvana Mernatnia, “Communication-efficient federated learning through adaptive weight clustering and server-side distillation,” in *2024 IEEE International Conference on Acoustics, Speech and Signal Processing (ICASSP)*, 2024, pp. 5805–5809.

[3] Martin Abadi, Andy Chu, Ian Goodfellow, H Brendan McMahan, Ilya Mironov, Kunal Talwar, and Li Zhang, “Deep learning with differential privacy,” in *Proceedings of the 2016 ACM SIGSAC Conference on Computer and Communications Security (CCS)*, 2016, pp. 308–318.

[4] Kang Wei, Jun Li, Ming Ding, Chuan Ma, Howard H Yang, Farhad Farokhi, Shi Jin, Tony QS Quek, and H Vincent Poor, “Federated learning with differential privacy: Algorithms and performance analysis,” *IEEE Transactions on Information Forensics and Security (TIFS)*, vol. 15, pp. 3454–3469, 2020.

[5] Florian Tramer and Dan Boneh, “Differentially private learning needs better features (or much more data),” in *Proceedings of the 9th International Conference on Learning Representations (ICLR)*, 2021, pp. 1–13.

[6] Robin Francis and Sundeep Prabhakar Chepuri, “Differentially private and communication-efficient decentralized learning using deep quantizers,” in *2025 IEEE International Conference on Acoustics, Speech and Signal Processing (ICASSP)*, 2025, pp. 1–5.

[7] Yuchen Yang, Bo Hui, Haolin Yuan, Neil Gong, and Yinzhi Cao, “{PrivateFL}: Accurate, differentially private federated learning via personalized data transformation,” in *Proceedings of the 32nd USENIX Conference on Security Symposium (USENIX Security)*, 2023, pp. 1595–1612.

[8] Ali Moradi Shahmiri, Chih Wei Ling, and Cheuk Ting Li, “Communication-efficient laplace mechanism for differential privacy via random quantization,” in *2024 IEEE International Conference on Acoustics, Speech and Signal Processing (ICASSP)*, 2024, pp. 4550–4554.

[9] Jiating Ma, Yipeng Zhou, Laizhong Cui, and Song Guo, “An optimized sparse response mechanism for differentially private federated learning,” *IEEE Transactions on Dependable and Secure Computing (TDSC)*, vol. 21, no. 4, pp. 2285–2295, 2023.

[10] Laizhong Cui, Jiating Ma, Yipeng Zhou, and Shui Yu, “Boosting accuracy of differentially private federated learning in industrial iot with sparse responses,” *IEEE Transactions on Industrial Informatics (TII)*, vol. 19, no. 1, pp. 910–920, 2022.

[11] Xuechen Li, Daogao Liu, Tatsunori B. Hashimoto, Huseyin A. Inan, Jarnardhan Kulkarni, Yin Tat Lee, and Abhradeep Guha Thakurta, “When does differentially private learning not suffer in high dimensions?,” in *Proceedings of the 36th International Conference on Neural Information Processing Systems (NeurIPS)*, 2022, pp. 2861–28630.

[12] Ergute Bao, Yangfan Jiang, Fei Wei, Xiaokui Xiao, Zitao Li, Yaliang Li, and Bolin Ding, “Unlocking the power of differentially private zeroth-order optimization for fine-tuning {LLMs},” in *Proceedings of the 34th USENIX Conference on Security Symposium (USENIX Security)*, 2025, pp. 1569–1588.

[13] Arun Ganesh, Mahdi Haghifam, Milad Nasr, Sewoong Oh, Thomas Steinke, Om Thakkar, Abhradeep Guha Thakurta, and Lun Wang, “Why is public pretraining necessary for private model training?,” in *Proceedings of the 40th International Conference on Machine Learning (ICML)*, 2023, pp. 10611–10627.

[14] Soham De, Leonard Berrada, Jamie Hayes, Samuel L Smith, and Borja Balle, “Unlocking high-accuracy differentially private image classification through scale,” *ArXiv Preprint ArXiv:2204.13650*, 2022.

[15] Chendi Wang, Yuqing Zhu, Weijie J Su, and Yu-Xiang Wang, “Neural collapse meets differential privacy: Curious behaviors of noisyGD with near-perfect representation learning,” in *Proceedings of the 41st International Conference on Machine Learning (ICML)*, 2024, pp. 52334–52360.

[16] Shuqi Ke, Charlie Hou, Giulia Fanti, and Sewoong Oh, “On the convergence of differentially-private fine-tuning: To linearly probe or to fully fine-tune?,” *ArXiv Preprint ArXiv:2402.18905*, 2024.

[17] Brendan McMahan and Seth Hampson Eider Moore, Daniel Ramage, “Communication-efficient learning of deep networks from decentralized data,” in *Proceedings of the 20th International Conference on Artificial Intelligence and Statistics (AISTATS)*, 2017, pp. 1273–1282.

[18] Yipeng Zhou, Xuezheng Liu, Yao Fu, Di Wu, Jessie Hui Wang, and Shui Yu, “Optimizing the numbers of queries and replies in convex federated learning with differential privacy,” *IEEE Transactions on Dependable and Secure Computing (TDSC)*, vol. 20, no. 6, pp. 4823–4837, 2023.

[19] Olga Russakovsky, Jia Deng, Hao Su, Jonathan Krause, Sanjeev Satheesh, Sean Ma, Zhiheng Huang, Andrej Karpathy, Aditya Khosla, Michael Bernstein, et al., “Imagenet large scale visual recognition challenge,” *International Journal of Computer Vision (IJCV)*, vol. 115, no. 3, pp. 211–252, 2015.

[20] Shiqiang Wang, Tiffany Tuor, Theodoros Salonidis, Kin K Leung, Christian Makaya, Ting He, and Kevin Chan, “Adaptive federated learning in resource constrained edge computing systems,” *IEEE Journal on Selected Areas in Communications (JSAC)*, vol. 37, no. 6, pp. 1205–1221, 2019.

[21] Mingzhe Chen, H Vincent Poor, Walid Saad, and Shuguang Cui, “Convergence time optimization for federated learning over wireless networks,” *IEEE Transactions on Wireless Communications*, vol. 20, no. 4, pp. 2457–2471, 2020.

[22] Debraj Basu, Deepesh Data, Can Karakus, and Suhas Diggavi, “Qsparse-local-sgd: Distributed sgd with quantization, sparsification and local computations,” *IEEE Journal on Selected Areas in Information Theory (JSAIT)*, vol. 1, no. 1, pp. 217–226, 2020.

[23] HarryChia-Hung Hsu, Hu Qi, and MatthewA. Brown, “Measuring the effects of non-identical data distribution for federated visual classification,” *ArXiv: Learning*, 2019.

[24] Kaiming He, Xiangyu Zhang, Shaoqing Ren, and Jian Sun, “Deep residual learning for image recognition,” in *Proceedings of the 2016 IEEE Conference on Computer Vision and Pattern Recognition (CVPR)*, 2016, pp. 770–778.

[25] Kaiming He, Xiangyu Zhang, Shaoqing Ren, and Jian Sun, “Delving deep into rectifiers: Surpassing human-level performance on imagenet classification,” in *Proceedings of the 2015 IEEE International Conference on Computer Vision (ICCV)*, 2015, pp. 1026–1034.